**Structural Engineering and Mechanics**, *Vol. 72, No. 1 (2019) 71-81*
DOI: https://doi.org/10.12989/sem.2019.72.1.071 

# Frequency response of initially deflected nanotubes conveying fluid via a nonlinear NSGT model

Ali Farajpour*[1,2], Mergen H. Ghayesh[1a] and Hamed Farokhi[2a]

[1]*School of Mechanical Engineering, University of Adelaide, South Australia 5005, Australia*
[2]*Department of Mechanical and Construction Engineering, Northumbria University, Newcastle upon Tyne NE1 8ST, UK*

*(Received April 11, 2019, Revised May 8, 2019, Accepted May 13, 2019)*

**Abstract.** The objective of this paper is to develop a size-dependent nonlinear model of beams for fluid-conveying nanotubes with an initial deflection. The nonlinear frequency response of the nanotube is analysed via an Euler-Bernoulli model. Size influences on the behaviour of the nanosystem are described utilising the nonlocal strain gradient theory (NSGT). Relative motions at the inner wall of the nanotube is taken into consideration via Beskok–Karniadakis model. Formulating kinetic and elastic energies and then employing Hamilton's approach, the nonlinear motion equations are derived. Furthermore, Galerkin's approach is employed for discretisation, and then a continuation scheme is developed for obtaining numerical results. It is observed that an initial deflection significantly alters the frequency response of NSGT nanotubes conveying fluid. For small initial deflections, a hardening nonlinearity is found whereas a softening-hardening nonlinearity is observed for large initial deflections.

**Keywords:** nonlinear frequency response; nanotubes; fluid flow; initial deflection

## 1. Introduction

Nanostructural components such as nanotubes and nanoplates form the basic blocks of many microelectromechanical and nanoelectromechanical systems. Salient examples of these systems are nanoscale/microscale generators, mass sensors and energy harvesters. Furthermore, nanostructures, especially carbon nanotubes and boron nitride nanotubes can be used for the reinforcement of composite plates (Bakhadda, Bouiadjra *et al*. 2018, Draoui, Zidour *et al*. 2019, Semmah, Heireche *et al*. 2019). Developing advanced mathematical modelling for understanding the mechanics of nanostructural components provides a platform to improve the performance of these ultrasmall systems.

Since the mechanical behaviour of ultrasmall structures such as graphene sheets and nanotubes is highly influenced by size effects (Ebrahimi and Barati 2018, Ebrahimi, Haghi *et al*. 2018, Nejad, Hadi *et al*. 2018, Farajpour, Ghayesh *et al*. 2019), the application of the classical continuum mechanics in analysing the mechanical behaviour at ultrasmall levels is not reliable. Therefore, the classical continuum mechanics is modified so as to capture size influences (Ebrahimi and Dabbagh 2018, Farajpour, Ghayesh *et al*. 2018, Arefi 2019, Benahmed, Fahsi *et al*. 2019, Gao, Xiao *et al*. 2019, Karami, Janghorban *et al*. 2019, Mohammadi and Rastgoo 2019, Nebab, Atmane *et al*. 2019). There are a number of size-dependent continuum-, Eringen's theory (Eringen and Edelen 1972, Farajpour, Shahidi *et al*. 2018) and strain gradient elasticity (Akgöz and Civalek 2013, Ghayesh, Amabili *et al*. 2013, Akgöz and Civalek 2014). In this work, a nonlocal theory incorporating strain gradient effects is used for deriving the motion equations of fluid-conveying nanotubes with an initial deflection.

In the last decade, for the first time, the application of the nonlocal theory to continuum modelling of nanoscale cantilevers was introduced by Peddieson *et al*. (Peddieson, Buchanan *et al*. 2003). Then, many investigations have been performed on the size-dependent continuum modelling of microscale fundamental components (Ghayesh, Amabili *et al*. 2013, Şimşek and Reddy 2013, Farokhi, Ghayesh *et al*. 2016, Farokhi and Ghayesh 2018) and nanoscale fundamental components (Reddy 2010, Farajpour, Rastgoo *et al*. 2017, Farajpour, Shahidi *et al*. 2018) via modifying the continuum mechanics. Various basic problems in solid mechanics at nanoscales such as wave propagation (Tounsi, Heireche *et al*. 2008), thermal buckling (Zenkour and Sobhy 2013), static deflection (Reddy 2010), resonance behaviour (Karami, Shahsavari *et al*. 2019) and vibration analysis with consideration of surface effects (Malekzadeh and Shojaee 2015) as well as homogeneous (Civalek and Akgöz 2013), inhomogeneous (Nejad, Hadi *et al*. 2017) and piezoelectric problems (Asemi and Farajpour 2014), have been studied.

Scale-dependent continuum formulations have been introduced for the mechanics of various types of small-scale structures involving nanoplates (Karami, Janghorban *et al*. 2017, Kadari, Bessaim *et al*. 2018), functionally graded nanoplates (Belkorissat, Houari *et al*. 2015, Bounouara, Benrahou *et al*. 2016, Besseghier, Houari *et al*. 2017, Khetir, Bouiadjra *et al*. 2017, Karami, Janghorban *et al*. 2018, Karami, Janghorban *et al*. 2018, Karami, Janghorban *et al*.

*Corresponding author, Ph.D. Student
E-mail: ali.farajpourouderji@adelaide.edu.au


http://www.techno-press.com/journals/sem&subpage=7 ISSN: 1225-4568 (Print), 1598-6217 (Online)

2018), graphene sheets (Bouadi, Bousahla *et al*. 2018, Bourada, Amara *et al*. 2018, Mokhtar, Heireche *et al*. 2018, Yazid, Heireche *et al*. 2018), nanobeams (Chaht, Kaci *et al*. 2015, Bellifa, Benrahou *et al*. 2017, Mouffoki, Bedia *et al*. 2017, Hamza-Cherif, Meradjah *et al*. 2018, Mokhtar, Heireche *et al*. 2018, Youcef, Kaci *et al*. 2018, Bedia, Houari *et al*. 2019), functionally graded nanobeams (Ahouel, Houari *et al*. 2016, Bouafia, Kaci *et al*. 2017), nanoshells (Karami, Janghorban *et al*. 2018), and nanoparticles (Karami, Janghorban *et al*. 2018) as well as microbeams (Al-Basyouni, Tounsi *et al*. 2015, Tlidji, Zidour *et al*. 2019).

Different higher-order theories have been utilised to capture scale influences on the mechanical response of small-scale structural components involving small-scale shells (Farokhi and Ghayesh 2018) and plates (Murmu and Adhikari 2013), panels (Demir, Mercan *et al*. 2016) as well as rods (Numanoğlu, Akgöz *et al*. 2018), beams (Zhang, He *et al*. 2014, Demir and Civalek 2017, Romano, Barretta *et al*. 2017) and tubes (Akgöz and Civalek 2011). Rahmani *et al*. (Rahmani, Refaeinejad *et al*. 2017) assessed different higher-order models with nonlocal influences for the static deformation and instability of functionally graded nanoscale beams; the inclusion of the influences of shear deformations results in a rise in deflection and a decrease in buckling force. Moreover, Akgoz and Civalek (Akgöz and Civalek 2017) examined the influences of shear deformations and temperature change on the vibrations of functionally graded nanoscale microbeams through use of a couple stress model. Malikan (Malikan 2017) also utilised a first-order theory of shear deformations for electromechanical stability analysis of smart nanoplates. In addition, scale-dependent higher-order models have been introduced for Silicon carbide nanotubes (Mercan and Civalek 2017) and boron nitride nanotubes (Mercan and Civalek 2016) as well as nanoscale beams resting on an elastic medium (Demir and Civalek 2017).

In addition to the size-dependent formulation and analysis of solid structural elements at small-scale levels, size effects on the mechanical behaviour of structural elements conveying fluid have been examined in the literature. For instance, the effects of a viscoelastic medium on the flow-induced stability and vibration of a single nanotube (Soltani, Taherian *et al*. 2010), the stability of nanotubes conveying pulsating fluid (Liang and Su 2013), and the flow-induced dynamics of nanotubes (Bahaadini, Saidi *et al*. 2018) as well as elastic waves in fluid-conveying both homogeneous and inhomogeneous nanotubes (Wang, Li *et al*. 2010, Filiz and Aydogdu 2015), have been analysed in recent times. Besides developing size-dependent formulation for fluid-conveying carbon nanotubes, other kinds of nanotubes including boron nitride (Maraghi, Arani *et al*. 2013) and piezoelectric nanotubes (Amiri, Talebitooti *et al*. 2018) conveying nanofluid have been taken into consideration.

As mentioned above, fluid-conveying nanotubes have mainly been analysed in terms of linear mechanics. Nonetheless, a few studies have been done with consideration of nonlinear strain components (Askari and Esmailzadeh 2017). More investigations are required in order to fully understand the nonlinear frequency response of nanotubes conveying fluid, especially when there is an initial deflection in the system. For the sake of simplification, the influences of an initial deflection on the frequency response of fluid-conveying tubes at nanoscales have not been examined yet. Initial deflections are very significant since in nanoscale electromechanical devices, the fundamental parts are very prone to initial thermomechanical loading, which can consequently cause initial deflections (Farokhi and Ghayesh 2015). In addition, in previous studies, the frequency response was calculated taking into consideration only one trial function for displacements. However, in this paper, a precise solution methodology is presented via consideration of a high number of trail functions.

The aim of this investigation is to examine the influences of an initial deflection on the nonlinear mechanical behaviour of NSGT nanotubes conveying nanofluid flow. A modified Euler-Bernoulli model with strain gradient and nonlocal effects is developed to examine the nonlinear frequency response. To model the relative motions at the inner wall of the nanotube, Beskok–Karniadakis model is also applied. Nonlinear motion equations are presented by formulating kinetic and elastic energies as well as employing Hamilton's approach. For accurately estimating the frequency response, firstly, a system with a high degree of freedom is developed based on Galerkin's approach. Secondly, a continuation method is implemented to extract numerical results in the time domain. The present results would help researchers and engineers with the design of nanoscale electromechanical devices involving nanotubes conveying flow.

## 2. A nonlocal strain gradient model for tubes conveying flow at nanoscales

Figure 1 shows the schematic configuration of an ultrasmall tube with an initial deflection, which is employed to convey flow at nanoscales. According to the Euler–Bernoulli model, one has the following relation for the nonlinear strain (Ghayesh 2018)

$$\varepsilon_{xx}=\frac{\partial u}{\partial x}-z\frac{\partial^2 w}{\partial x^2}+\frac{\partial w}{\partial x}\frac{dw_0}{dx}+\frac{1}{2}\left(\frac{\partial w}{\partial x}\right)^2 \tag{1}$$

Here the initial deflection, transverse and axial displacements are denoted by $w_0$, $w$ and $u$, respectively. The NSGT-based constitutive relation of nanotubes is given by (Şimşek 2016)

$$t_{xx}-\left(e_0 a\right)^2\nabla^2 t_{xx}=t_{xx}^{cl}-l_{sg}^2\nabla^2 t_{xx}^{cl}, \tag{2}$$

where

$$t_{xx}^{cl}=E\varepsilon_{xx} \tag{3}$$

where $t_{xx}^{cl}$ indicates the classical stress, and $t_{xx}$ is the total stress; $l_{sg}$, $E$ and $e_0 a$ represent the scale parameter linked

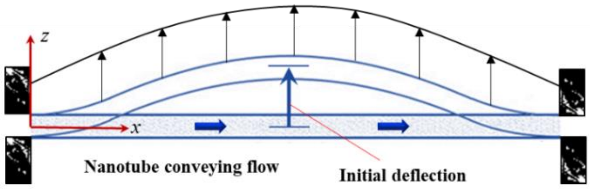


Fig. 1 An initial deflection in a nanotube conveying flow

to strain gradients, elasticity modulus and the scale parameter linked to stress nonlocality, respectively. In the nonlocal parameter, $e_0$ is a coefficient, which is employed to calibrate the theoretical model, and $a$ is an internal characteristic size of nanotubes (Mohammadi *et al*. 2014, Farajpour *et al*. 2018, Mohammadi *et al*. 2013, farajpour *et al*. 2019, Malekzadeh *et al*. 2012, Farajpour *et al*. 2019). For instance, the internal characteristic size of carbon nanotubes is the bond length between two adjacent carbons. In this case, for the Laplace operator, one has $\nabla^2()=\partial^2()/\partial x^2$. Furthermore, let us consider $I$ and $A$ as the inertia moment and area of cross-section.

The force and moment resultants are

$$\langle N_{xx}, M_{xx}\rangle = \int_A \langle 1, z\rangle t_{xx} dA. \tag{4}$$

In view of the above equations, the force and moment resultants are written as

$$\begin{aligned} N_{xx} &= EA\left(1-l_{sg}^2\nabla^2\right)\left[\frac{1}{2}\left(\frac{\partial w}{\partial x}\right)^2+\frac{\partial u}{\partial x}\right] \\ &+EA\left(1-l_{sg}^2\nabla^2\right)\left[\frac{\partial w}{\partial x}\frac{dw_0}{dx}\right]+\left(e_0a\right)^2\nabla^2 N_{xx}, \end{aligned} \tag{5}$$

$$M_{xx} = -EI\left(1-l_{sg}^2\nabla^2\right)\left[\frac{\partial^2 w}{\partial x^2}\right]+\left(e_0a\right)^2\nabla^2 M_{xx} \tag{6}$$

Based on the NSGT, the elastic energy is (Lim, Zhang *et al*. 2015, Şimşek 2016)

$$\delta U_{el} = \int_0^L\int_A \sigma_{xx}\delta\varepsilon_{xx} dA dx + \int_0^L\int_A \sigma_{xx}^{(1)}\nabla\delta\varepsilon_{xx} dA dx, \tag{7}$$

where the lower- and first-order non-classical stresses are indicated by $\sigma_{xx(\alpha\beta)}$ and $\sigma^{(1)}_{xx(\alpha\beta)}$ represent, respectively; also, $L$ represents the tube length. Assuming $\nabla$ as the gradient operator, the lower- and first-order non-classical stresses are related as (Lim, Zhang *et al*. 2015)

$$t_{xx} = \sigma_{xx} - \nabla\sigma_{xx}^{(1)} \tag{8}$$

Taking into account the effect of the relative motion at the inner wall, the total kinetic energy is obtained as (Paidoussis 1998)

$$\begin{aligned} T_k &= \frac{1}{2}\rho_t\int_A\int_0^L\left(\left(\frac{\partial u}{\partial t}\right)^2+\left(\frac{\partial w}{\partial t}\right)^2\right)dAdx \\ &+\frac{1}{2}\rho_f\int_A\int_0^L\left(\left[\frac{\partial u}{\partial t}+\kappa_{scf}U\left(1+\frac{\partial u}{\partial x}\right)\right]^2+\right. \\ &\left.+\left[\frac{\partial w}{\partial t}+\kappa_{scf}U\left(\frac{\partial w}{\partial x}+\frac{dw_0}{dx}\right)\right]^2\right)dAdx. \end{aligned} \tag{9}$$

In Eq. (20), $\kappa_{scf}$ is the speed correction factor; $\rho$ and $U$ are, respectively, the mass density and fluid speed; "$t$" and "$f$" are abbreviations for "tube" and "fluid", respectively. Assuming $F(x)$ as the amplitude of applied loading and $\omega$ as the excitation frequency of applied loading, the external work is

$$\delta W_F = \int_0^L F(x)\cos(\omega t)\delta w\, dx. \tag{10}$$

Using Eqs. (7), (9) and (10) together with the following principle

$$\int_{t_1}^{t_2}\left\{\delta W_F+\delta T_k-\delta U_{el}\right\}dt = 0, \tag{11}$$

the nanotube motion equations are derived as

$$(M+m)\frac{\partial^2 u}{\partial t^2}+M\left(\kappa_{scf}U\right)^2\frac{\partial^2 u}{\partial x^2}+2M\left(\kappa_{scf}U\right)\frac{\partial^2 u}{\partial t\partial x}-\frac{\partial N_{xx}}{\partial x}=0 \tag{12}$$

$$\begin{aligned} &(M+m)\frac{\partial^2 w}{\partial t^2}+M\left(\kappa_{scf}U\right)^2\left(\frac{\partial^2 w}{\partial x^2}+\frac{d^2 w_0}{dx^2}\right) \\ &+2M\left(\kappa_{scf}U\right)\frac{\partial^2 w}{\partial t\partial x}-F(x)\cos(\omega t)-\frac{\partial}{\partial x}\left(N_{xx}\frac{dw_0}{dx}\right) \\ &-\frac{\partial}{\partial x}\left(N_{xx}\frac{\partial w}{\partial x}\right)-\frac{\partial^2 M_{xx}}{\partial x^2}=0, \end{aligned} \tag{13}$$

in which $M$ is the mass of fluid per length while $m$ denotes the mass of the tube per length (Ghayesh *et al*. 2019, Farajpour *et al*. 2018, Ghayesh *et al*. 2019, Farajpour *et al*. 2019). To derive the differential equations in terms of displacement components, Eqs. (12) and (13) are used together with Eqs. (5) and (6). The derived coupled nonlinear equations are as

$$\begin{aligned} &\left(1-\left(e_0a\right)^2\nabla^2\right)\left[(M+m)\frac{\partial^2 u}{\partial t^2}\right. \\ &\left.+M\left(\kappa_{scf}U\right)^2\frac{\partial^2 u}{\partial x^2}+2M\left(\kappa_{scf}U\right)\frac{\partial^2 u}{\partial t\partial x}\right] \\ &-EA\left(1-l_{sg}^2\nabla^2\right)\left[\frac{\partial w}{\partial x}\frac{\partial^2 w}{\partial x^2}+\frac{\partial^2 u}{\partial x^2}\right] \\ &-EA\left(1-l_{sg}^2\nabla^2\right)\left[\frac{dw_0}{dx}\frac{\partial^2 w}{\partial x^2}+\frac{d^2 w_0}{dx^2}\frac{\partial w}{\partial x}\right]=0, \end{aligned} \tag{14}$$

$$\begin{aligned} &\cos(\omega t)\left[F(x)-\left(e_0a\right)^2\frac{d^2F(x)}{dx^2}\right]+EI\left[l_{sg}^2\frac{\partial^6 w}{\partial x^6}-\frac{\partial^4 w}{\partial x^4}\right] \\ &+\left[EA\left(1-\left(e_0a\right)^2\nabla^2\right)\right]\left(\left[\frac{d^2 w_0}{dx^2}+\frac{\partial^2 w}{\partial x^2}\right]\left(1-l_{sg}^2\nabla^2\right)\times\right. \\ &\left.\left[\frac{dw_0}{dx}\frac{\partial w}{\partial x}+\frac{1}{2}\left(\frac{\partial w}{\partial x}\right)^2+\frac{\partial u}{\partial x}\right]\right)+\left[EA\left(1-\left(e_0a\right)^2\nabla^2\right)\right]\times \\ &\left(\left[\frac{dw_0}{dx}+\frac{\partial w}{\partial x}\right]\left[\frac{\partial}{\partial x}\left(\left(1-l_{sg}^2\nabla^2\right)\left[\frac{\partial w}{\partial x}\frac{dw_0}{dx}+\frac{1}{2}\left(\frac{\partial w}{\partial x}\right)^2+\frac{\partial u}{\partial x}\right]\right)\right]\right) \\ &+\left[\left(e_0a\right)^2\left(1-\left(e_0a\right)^2\nabla^2\right)\right]\left(\left[\frac{\partial^2 w}{\partial x^2}+\frac{d^2 w_0}{dx^2}\right]\times\right. \end{aligned} \tag{15}$$

$$\left[\left(M+m\right)\frac{\partial^3 u}{\partial x\partial t^2}+M\left(\kappa_{scf}U\right)^2\frac{\partial^3 u}{\partial x^3}+2M\left(\kappa_{scf}U\right)\frac{\partial^3 u}{\partial t\partial x^2}\right]\Bigg)$$
$$+\left[\left(e_0a\right)^2\left(1-\left(e_0a\right)^2\nabla^2\right)\right]\left(\left[\frac{\partial w}{\partial x}+\frac{dw_0}{dx}\right]\times\right.$$
$$\left[\left(M+m\right)\frac{\partial^4 u}{\partial x^2\partial t^2}+2M\left(\kappa_{scf}U\right)\frac{\partial^4 u}{\partial t\partial x^3}+M\left(\kappa_{scf}U\right)^2\frac{\partial^4 u}{\partial x^4}\right]\Bigg)$$
$$=\left(M+m\right)\frac{\partial^2 w}{\partial t^2}+M\left(\kappa_{scf}U\right)^2\left(\frac{\partial^2 w}{\partial x^2}+\frac{d^2 w_0}{dx^2}\right)$$
$$+2M\left(\kappa_{scf}U\right)\frac{\partial^2 w}{\partial t\partial x}-\left(e_0a\right)^2\left[\left(M+m\right)\frac{\partial^4 w}{\partial x^2\partial t^2}\right.$$
$$\left.+M\left(\kappa_{scf}U\right)^2\left(\frac{\partial^4 w}{\partial x^4}+\frac{d^4 w_0}{dx^4}\right)+2M\left(\kappa_{scf}U\right)\frac{\partial^4 w}{\partial t\partial x^3}\right].$$

## 3. Solution technique

To obtain the frequency response of fluid-conveying nanotubes with an initial deflection, a numerical solution technique is developed in this section based on continuation and Galerkin methods (Ghayesh 2012, Kazemirad *et al.* 2013, Farokhi and Ghayesh 2017, Ghayesh *et al.* 2015, Farokhi *et al.* 2017). First of all, a set of dimensionless parameters is introduced as

$$\begin{gathered}x^*=\frac{x}{L},\ \varphi_{sg}=\frac{l_{sg}}{L},\ \varphi_{nl}=\frac{e_0a}{L},\ w_0^*=\frac{w_0}{d},\ u^*=\frac{u}{d},\\ w^*=\frac{w}{d},\ \Xi=L^2\frac{A}{I},\ s=\frac{L}{d},\ F^*=\frac{L^4}{EId}F,\ U^*=L\left(\sqrt{\frac{M}{EI}}\right)U,\\ \omega^*=L^2\left(\sqrt{\frac{m+M}{EI}}\right)\omega,\ \Pi_m=\frac{M}{M+m},\ t^*=\frac{1}{L^2}\left(\sqrt{\frac{EI}{m+M}}\right)t.\end{gathered}\tag{16}$$

where $d$ is the outer diameter of the nanotube. Moreover, in the present work, $h$ and $R$ are employed to indicate the thickness and outer radius, respectively. Using Eq. (16), the motion equations are first rewritten in a non-dimensional form. Then, applying Galerkin's procedure (Ghayesh and Farokhi 2015, Ghayesh 2018, Ghayesh 2018), the following expressions are used for the sake of discretisation

$$\begin{aligned}u\left(x,t\right)&=\sum_{j=1}^{N_x}\phi_j\left(x\right)r_j\left(t\right),\\ w\left(x,t\right)&=\sum_{j=1}^{N_z}\psi_j\left(x\right)q_j\left(t\right),\end{aligned}\tag{17}$$

in which ($r_j$, $\phi_j$)=(axial generalised coordinate, axial trial function) and ($q_j$, $\psi_j$)=(transverse generalised coordinate, transverse trial function) (Gholipour, Farokhi *et al.* 2015, Ghayesh, Farokhi *et al.* 2016). A clamped-clamped nanotube with an initial deflection in the form of $w_0=A_0\psi_1(x)$ is considered; $A_0$ denotes the initial deflection coefficient. Employing Eqs. (16) and (17) together with Eqs. (14) and (15) gives

$$\begin{aligned}&\left(\frac{s}{\Xi}\right)\left\{\sum_{j=1}^{N_x}\ddot{r}_j\left(\int_0^1\phi_k\phi_j dx\right)+\left(\kappa_{scf}U\right)^2\sum_{j=1}^{N_x}r_j\left(\int_0^1\phi_k\left(\phi_j\right)''dx\right)\right.\\ &\left.+2\left(\kappa_{scf}U\right)\sqrt{\Pi_m}\sum_{j=1}^{N_x}\dot{r}_j\left(\int_0^1\phi_k\left(\phi_j\right)'dx\right)\right\}-\left(\frac{s}{\Xi}\right)\varphi_{nl}^2\times\\ &\left\{\sum_{j=1}^{N_x}\ddot{r}_j\left(\int_0^1\phi_k\left(\phi_j\right)''dx\right)+\left(\kappa_{scf}U\right)^2\sum_{j=1}^{N_x}r_j\left(\int_0^1\phi_k\left(\phi_j\right)''''dx\right)\right.\\ &\left.+2\left(\kappa_{scf}U\right)\sqrt{\Pi_m}\sum_{j=1}^{N_x}\dot{r}_j\left(\int_0^1\phi_k\left(\phi_j\right)'''dx\right)\right\}\\ &-\int_0^1\left\{\phi_k\begin{bmatrix}A_0\sum_{j=1}^{N_z}\left(\psi_1\right)'\left(\psi_j\right)'q_j+s\sum_{j=1}^{N_x}\left(\phi_j\right)'r_j\\ +\frac{1}{2}\sum_{j=1}^{N_z}\sum_{i=1}^{N_z}\left(\psi_j\right)'\left(\psi_i\right)'q_jq_i\end{bmatrix}'\right\}dx\\ &+\varphi_{sg}^2\int_0^1\left\{\phi_k\begin{bmatrix}A_0\sum_{j=1}^{N_z}\left(\psi_1\right)'\left(\psi_j\right)'q_j+s\sum_{j=1}^{N_x}\left(\phi_j\right)'r_j\\ +\frac{1}{2}\sum_{j=1}^{N_z}\sum_{i=1}^{N_z}\left(\psi_j\right)'\left(\psi_i\right)'q_jq_i\end{bmatrix}'''\right\}dx=0,\end{aligned}\tag{18}$$

$$\begin{aligned}&\sum_{j=1}^{N_z}\left(\int_0^1\psi_k\psi_j dx\right)\ddot{q}_j+2\left(\kappa_{scf}U\right)\sqrt{\Pi_m}\sum_{j=1}^{N_z}\left(\int_0^1\psi_k\left(\psi_j\right)'dx\right)\dot{q}_j\\ &+\left(\kappa_{scf}U\right)^2\left[\sum_{j=1}^{N_z}\left(\int_0^1\psi_k\left(\psi_j\right)''dx\right)q_j+A_0\left(\int_0^1\psi_k\left(\psi_1\right)''dx\right)\right]-\varphi_{nl}^2\times\\ &\left\{\sum_{j=1}^{N_z}\left(\int_0^1\psi_k\left(\psi_j\right)''dx\right)\ddot{q}_j+2\left(\kappa_{scf}U\right)\sqrt{\Pi_m}\sum_{j=1}^{N_z}\left(\int_0^1\psi_k\left(\psi_j\right)'''dx\right)\dot{q}_j\right.\\ &\left.+\left(\kappa_{scf}U\right)^2\left[\sum_{j=1}^{N_z}\left(\int_0^1\psi_k\left(\psi_j\right)''''dx\right)q_j+A_0\left(\int_0^1\psi_k\left(\psi_1\right)''''dx\right)\right]\right\}-\varphi_{sg}^2\times\\ &\sum_{j=1}^{N_z}\left(\int_0^1\psi_k\left(\psi_j\right)^{(6)}dx\right)q_j-\left(\int_0^1\psi_k dx\right)F_1\cos\left(\omega t\right)+\sum_{j=1}^{N_z}\left(\int_0^1\psi_k\left(\psi_j\right)''''dx\right)q_j\\ &-\Xi\left(\frac{1}{s}\right)^2\int_0^1\left(\psi_k\left\{\left(\sum_{j=1}^{N_z}\left(\psi_j\right)''q_j+A_0\left(\psi_1\right)''\right)\left[\frac{1}{2}\sum_{j=1}^{N_z}\sum_{i=1}^{N_z}\left(\psi_j\right)'\left(\psi_i\right)'q_jq_i\right.\right.\right.\\ &\left.+s\sum_{j=1}^{N_x}\left(\phi_j\right)'r_j+A_0\sum_{j=1}^{N_z}\left(\psi_1\right)'\left(\psi_j\right)'q_j\right]+\left(\sum_{j=1}^{N_z}\left(\psi_j\right)'q_j+A_0\left(\psi_1\right)'\right)\times\\ &\left[s\sum_{j=1}^{N_x}\left(\phi_j\right)'r_j+A_0\sum_{j=1}^{N_z}\left(\psi_1\right)'\left(\psi_j\right)'q_j+\frac{1}{2}\sum_{j=1}^{N_z}\sum_{i=1}^{N_z}\left(\psi_j\right)'\left(\psi_i\right)'q_jq_i\right]'\\ &-\varphi_{sg}^2\left(\sum_{j=1}^{N_z}\left(\psi_j\right)''q_j+A_0\left(\psi_1\right)''\right)\left[s\sum_{j=1}^{N_x}\left(\phi_j\right)'r_j+A_0\sum_{j=1}^{N_z}\left(\psi_1\right)'\left(\psi_j\right)'q_j\right.\\ &\left.+\frac{1}{2}\sum_{j=1}^{N_z}\sum_{i=1}^{N_z}\left(\psi_j\right)'\left(\psi_i\right)'q_jq_i\right]''-\varphi_{sg}^2\left(\sum_{j=1}^{N_z}\left(\psi_j\right)'q_j+A_0\left(\psi_1\right)'\right)\times\\ &\left[s\sum_{j=1}^{N_x}\left(\phi_j\right)'r_j+\frac{1}{2}\sum_{j=1}^{N_z}\sum_{i=1}^{N_z}\left(\psi_j\right)'\left(\psi_i\right)'q_jq_i+A_0\sum_{j=1}^{N_z}\left(\psi_1\right)'\left(\psi_j\right)'q_j\right]'''\\ &+\left(\frac{s}{\Xi}\right)\varphi_{nl}^2\left(A_0\left(\psi_1\right)''+\sum_{j=1}^{N_z}q_j\left(\psi_j\right)''\right)\left[\left(\kappa_{scf}U\right)^2\sum_{j=1}^{N_x}r_j\left(\phi_j\right)'''\right.\\ &\left.+\sum_{j=1}^{N_x}\ddot{r}_j\left(\phi_j\right)'+2\left(\kappa_{scf}U\right)\sqrt{\Pi_m}\sum_{j=1}^{N_x}\dot{r}_j\left(\phi_j\right)''\right]\end{aligned}\tag{19}$$

$$+\left(\frac{s}{\Xi}\right)\varphi_{nl}^{2}\left(A_0\left(\psi_1\right)'+\sum_{j=1}^{N_z}q_j\left(\psi_j\right)'\right)\left[\sum_{j=1}^{N_x}\ddot{r}_j\left(\phi_j\right)''+\right.$$

$$\left.\left.\left.\left(\kappa_{scf}U\right)^2\sum_{j=1}^{N_x}r_j\left(\phi_j\right)''''+2\left(\kappa_{scf}U\right)\sqrt{\Pi_m}\sum_{j=1}^{N_x}\dot{r}_j\left(\phi_j\right)'''\right]\right\}\right)dx$$

$$+\Xi\left(\frac{\varphi_{nl}}{s}\right)^2\int_0^1\left(\psi_k\left\{\left(A_0\left(\psi_1\right)''+\sum_{j=1}^{N_z}q_j\left(\psi_j\right)''\right)\times\right.\right.$$

$$\left[s\sum_{j=1}^{N_x}r_j\left(\phi_j\right)'+\frac{1}{2}\sum_{j=1}^{N_z}\sum_{i=1}^{N_z}q_jq_i\left(\psi_j\right)'\left(\psi_i\right)'+A_0\sum_{j=1}^{N_z}q_j\left(\psi_1\right)'\left(\psi_j\right)'\right]$$

$$+\left(A_0\left(\psi_1\right)'+\sum_{j=1}^{N_z}\left(\psi_j\right)'q_j\right)\left[s\sum_{j=1}^{N_x}r_j\left(\phi_j\right)'+A_0\sum_{j=1}^{N_z}q_j\left(\psi_1\right)'\left(\psi_j\right)'\right.$$

$$\left.+\frac{1}{2}\sum_{j=1}^{N_z}\sum_{i=1}^{N_z}q_jq_i\left(\psi_j\right)'\left(\psi_i\right)'\right]'-\varphi_{sg}^2\left(A_0\left(\psi_1\right)''+\sum_{j=1}^{N_z}q_j\left(\psi_j\right)''\right)\times$$

$$\left[s\sum_{j=1}^{N_x}r_j\left(\phi_j\right)'+A_0\sum_{j=1}^{N_z}\left(\psi_1\right)'\left(\psi_j\right)'q_j+\frac{1}{2}\sum_{j=1}^{N_z}\sum_{i=1}^{N_z}q_jq_i\left(\psi_j\right)'\left(\psi_i\right)'\right]''$$

$$-\varphi_{sg}^2\left(A_0\left(\psi_1\right)'+\sum_{j=1}^{N_z}q_j\left(\psi_j\right)'\right)\left[A_0\sum_{j=1}^{N_z}q_j\left(\psi_1\right)'\left(\psi_j\right)'\right.$$

$$\left.+s\sum_{j=1}^{N_x}\left(\phi_j\right)'r_j+\frac{1}{2}\sum_{j=1}^{N_z}\sum_{i=1}^{N_z}q_jq_i\left(\psi_j\right)'\left(\psi_i\right)'\right]'''$$

$$+\left(\frac{s}{\Xi}\right)\varphi_{nl}^2\left(A_0\left(\psi_1\right)''+\sum_{j=1}^{N_z}q_j\left(\psi_j\right)''\right)\left[\left(\kappa_{scf}U\right)^2\sum_{j=1}^{N_x}r_j\left(\phi_j\right)'''\right.$$

$$\left.+\sum_{j=1}^{N_x}\ddot{r}_j\left(\phi_j\right)'+2\left(\kappa_{scf}U\right)\sqrt{\Pi_m}\sum_{j=1}^{N_x}\dot{r}_j\left(\phi_j\right)''\right]$$

$$+\left(\frac{s}{\Xi}\right)\varphi_{nl}^2\left(A_0\left(\psi_1\right)'+\sum_{j=1}^{N_z}q_j\left(\psi_j\right)'\right)\times\left[\sum_{j=1}^{N_x}\ddot{r}_j\left(\phi_j\right)''+\right.$$

$$\left.\left.\left.\left(\kappa_{scf}U\right)^2\sum_{j=1}^{N_x}r_j\left(\phi_j\right)''''+2\left(\kappa_{scf}U\right)\sqrt{\Pi_m}\sum_{j=1}^{N_x}\dot{r}_j\left(\phi_j\right)'''\right]'\right\}\right)dx=0.$$

The superscript "*" is neglected for convenience. From Eqs. (18) and (19), a set of discretised coupled differential equations is obtained. The resultant differential equations are numerically solved by a continuation method (Farokhi and Ghayesh 2018, Ghayesh and Farajpour 2018).

## 4. Results and discussion

Numerical results are presented in the following section for a clamped-clamped nanosystem with 20 degrees of freedom (ten degrees of freedom along each direction). The tube mass density, Poisson's ratio and Young's constant are 1024 kg/m$^3$, 0.3 and 610 MPa, respectively (Shen 2011). These material properties belong to small-scale lipid tubules, which are a class of soft ultrasmall tubes. A dimensionless damping coefficient ($c_d$=0.25) is introduced in the calculation. Furthermore, the tube geometric features are $h$=66.0 nm, $R$=290.5 nm, and $L/d$=20. The dimensionless parameters are $\kappa_{scf}$=1.0788, $\Pi_m$=0.5915, $\Xi$=4006.9411, $\varphi_{sg}$ = 0.04 and $\varphi_{nl}$ = 0.08.

The nonlinear frequency response of nanotubes with an initial deflection conveying flow is illustrated in Fig. 2 for $U$=3.65, $\kappa_{scf}$=1.0788, $A_0$=0.10, $F_1$=2.5, and $\omega_1$=16.3803. The maximum values of $u$ and $w$ are plotted versus the frequency ratio (excitation frequency/natural frequency). A hardening-type frequency response involving two distinct bifurcation points at $\omega/\omega_1$=1.1194 and 1.0238 is observed. In addition, slight modal interactions are seen in the nonlinear frequency response of the nanotube around $\omega/\omega_1$ =1.0171 for motions in both directions. Figures 3 and 4 indicates the total transverse displacement of the nanotube in one oscillation period for two important cases, namely when modal interactions are strongest and at peak oscillation amplitude, respectively.

Table 1 Verification study for the linear vibration of simply-supported nanoscale tubes

| Mode number | Classical model | Strain gradient model | Nonlocal model | NSGT (present) | NSGT (Li, Li *et al.* 2017) |
|---|---|---|---|---|---|
| 1 | 9.8696 | 9.9906 | 9.8502 | 9.9710 | 9.97 |
| 2 | 39.4784 | 41.3808 | 39.1704 | 41.0579 | 41.06 |
| 3 | 88.8264 | 98.1951 | 87.2893 | 96.4957 | 96.50 |
| 4 | 157.9137 | 186.4976 | 153.1508 | 180.8726 | 180.87 |

First of all, the accuracy and validity of the present model are demonstrated in Table 1 by making a comparison between the obtained results and those available in the literature for the frequencies values of uniform nanobeams. The difference between the nonlocal, classical, NSGT and strain gradient models can be calculated from this table. For nonlocal, classical, NSGT and strain gradient models, scale parameters are set to $<\varphi_{sg},\varphi_{nl}>$ = <0,0,02>, $<\varphi_{sg},\varphi_{nl}>$ = <0,0>, $<\varphi_{sg},\varphi_{nl}>$ = <0.05,0.02> and $<\varphi_{sg},\varphi_{nl}>$ = <0.05,0>. respectively. For an appropriate comparison, the features of the nanobeam are the same as those assumed in Ref. (Li, Li *et al.* 2017). From the table, a reasonable agreement is observed, demonstrating the validity of the proposed modelling. Moreover, the strain gradient model leads to the highest dimensionless frequencies $(\omega^*=\omega\sqrt{\rho L^2/E})$ whereas the smallest ones are obtained by the nonlocal model.

The physical explanation for the observed increase in the frequency parameter with increasing strain gradient influence is that the stiffness of structural components at ultrasmall levels is related to strain gradients. The stiffness is higher for stronger strain gradient influences, and this causes the tube to vibrate at a higher natural frequency. However, the nonlocal influence makes the nanosystem experience lower frequency parameters. The physical explanation for this phenomenon is rooted in the reduction of structural stiffness with enhancing nonlocal influences.

The influence of an initial deflection on the nonlinear frequency response of the nanotube conveying flow is illustrated in Fig. 5 for $U$=4.0 and $F_1$=2.5. This figure reveals the importance of the consideration of the initial deflection on the frequency response. When there is a slight initial deflection in the nanotube, a hardening-type nonlinearity governs the frequency response. Nonetheless, for larger initial deflections, the frequency response is governed by a softening-hardening response. In fact, the nonlinear frequency response of the system can be tailored by creating an initial deflection during manufacturing

(a)

(b)

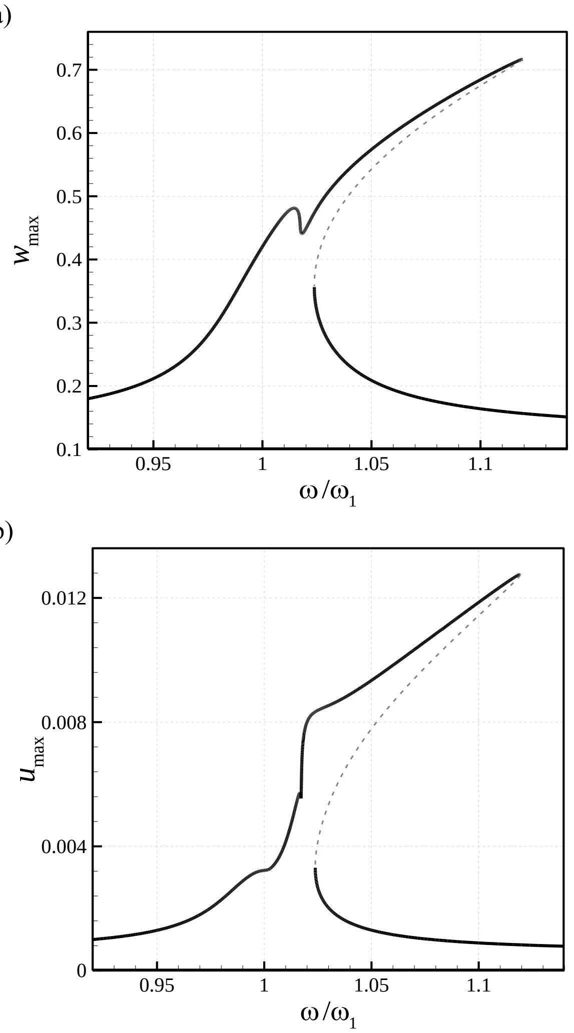


Fig. 2 Nonlinear frequency response of the nanotube; (a) $w_{max}$ at $x$=0.5; (b) $u_{max}$ at $x$=0.66; dashed line: unstable branch; solid line: stable branch.

process. This is important in ultrasmall electromechanical systems in which there is a fluid-conveying nanotube. Another significant finding is that modal interactions, which are found in the frequency response for small initial deflections (especially, for the axial motion), can be removed by creating higher initial deflections in the nanotube.

The significance of size effects on the coupled nonlinear frequency response of the nanotube conveying flow is indicated in Fig. 6. The initial deflection coefficient and flow speed are, respectively, $A_0$=0.15 and $U$=4.0. The speed correction coefficient and the amplitude of applied loading are set to $\kappa_{scf}$=1.0788 and $F_1$=3.0, respectively. The frequency response is plotted for the classical theory (CT) and NSGT. In the CT, size effects are neglected (i.e. $\varphi_{sg}$ = 0.0 and $\varphi_{nl}$ = 0.0) while the size parameters of the NSGT are set to $\varphi_{sg}$ = 0.04 and $\varphi_{nl}$ = 0.08. The resonance frequency of the CT is noticeably higher than that of the NSGT due to the decreasing effect of stress nonlocality on the stiffness. In addition, the CT overestimates modal interactions, especially for the axial motion.

Figures 7 and 8 illustrate the nonlinear coupled

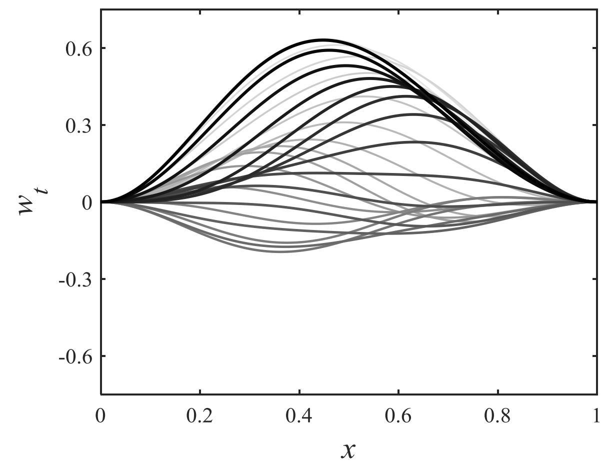


Fig. 3 Total transverse displacement ($w_t$=$w$+$w_0$) of the fluid-conveying nanotube of Fig. 2 in one period of oscillation at $\omega/\omega_1$ = 1.0171 (i.e. when modal interactions are strongest).

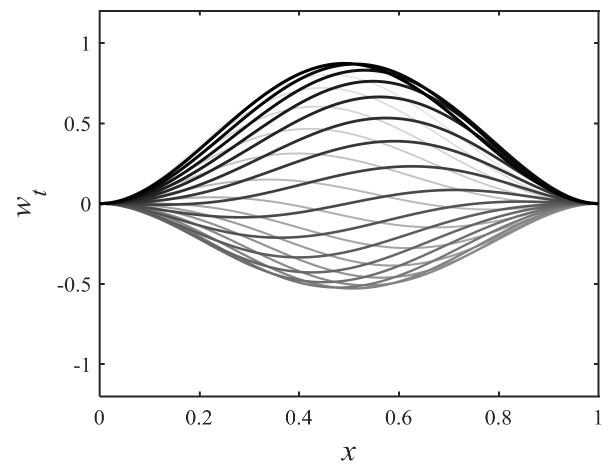


Fig. 4 Total transverse displacement ($w_t$=$w$+$w_0$) of the fluid-conveying nanotube of Fig. 2 in one period of oscillation at $\omega/\omega_1$ = 1.1194 (i.e. at peak oscillation amplitude).

frequency response of the nanotube conveying flow for slip and no-slip conditions. In both figures, the initial deflection coefficient and the amplitude of applied loading are assumed as $A_0$=0.15 and $F_1$=2.5, respectively. In Fig. 7, the flow speed is set to $U$=3.0 whereas a value of 6.50 is considered for the dimensionless flow speed in Fig. 8. Depending on the flow speed, slip condition effect can increase or decrease the resonance frequency. When the flow speed is $U$=3.0, slip effects result in a reduction in the resonance frequency whereas relative motions at the wall are associated with a substantial increase in the resonance frequency for higher flow speed.

## 5. Conclusions

This paper dealt with the development of a size-dependent nonlinear model for nanotubes conveying flow when there is an initial deflection in the geometry. The Euler-Bernoulli model was applied in conjunction with the NSGT for formulating the nonlinear frequency response of

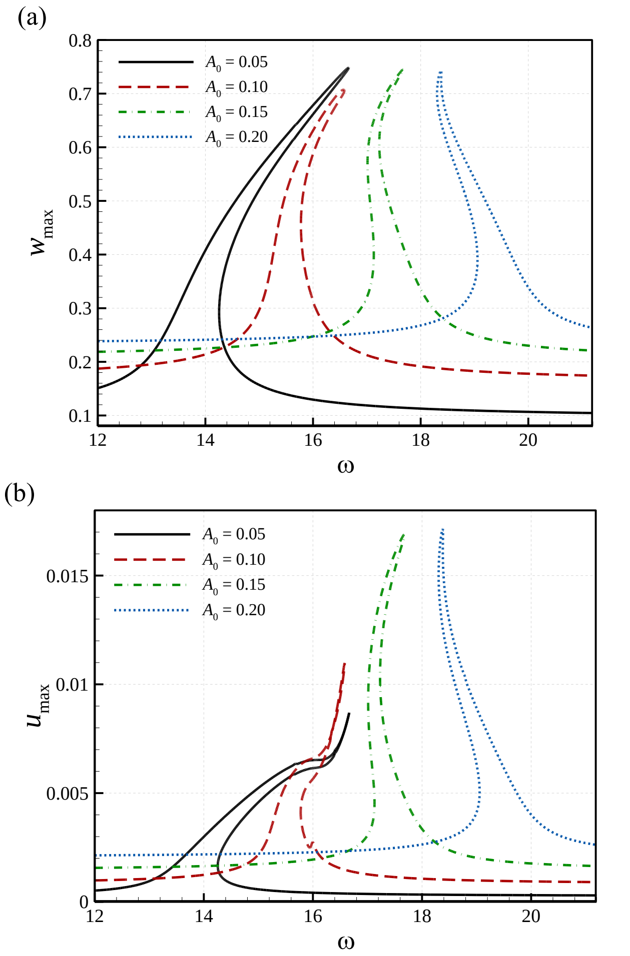


Fig. 5 Effect of an initial deflection on the nonlinear frequency response of the nanotube conveying flow; (a) $w_{max}$ at $x$=0.5 (b) $u_{max}$ at $x$=0.66

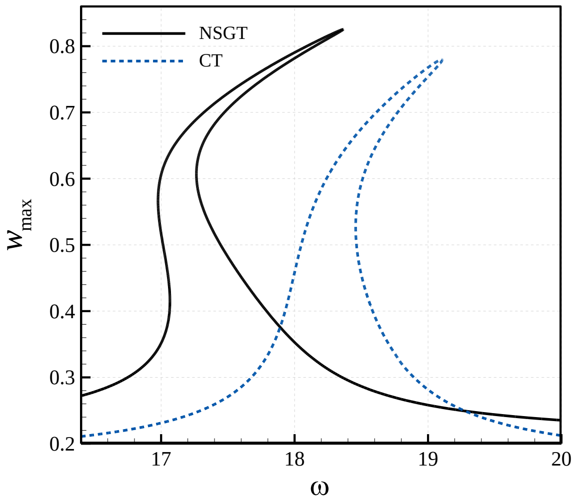


Fig. 6 Nonlinear frequency response of the nanotube conveying flow based on the CT and NSGT for $w_{max}$ at $x$=0.5

the nanosystem. To capture slip effects on the nonlinear coupled motion, the Beskok–Karniadakis model was used. Formulating kinetic and elastic energies and applying Hamilton's approach, the nonlinear motion equations were

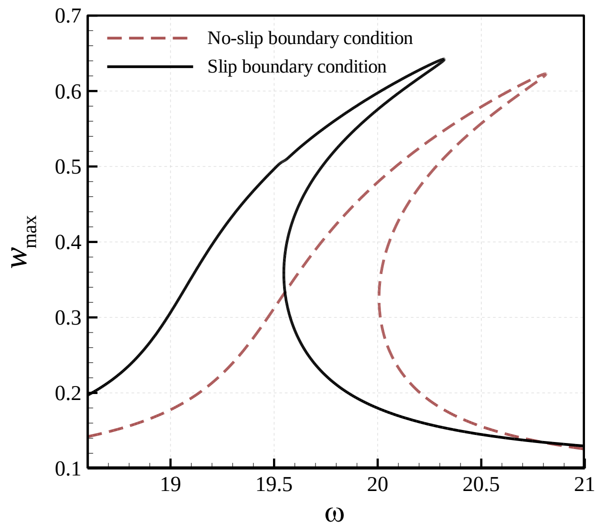


Fig. 7. Nonlinear frequency response of the nanosystem for slip and no-slip conditions for $w_{max}$ at $x$=0.5; $U$=3.0, $A_0$=0.15 and $F_1$=2.5.

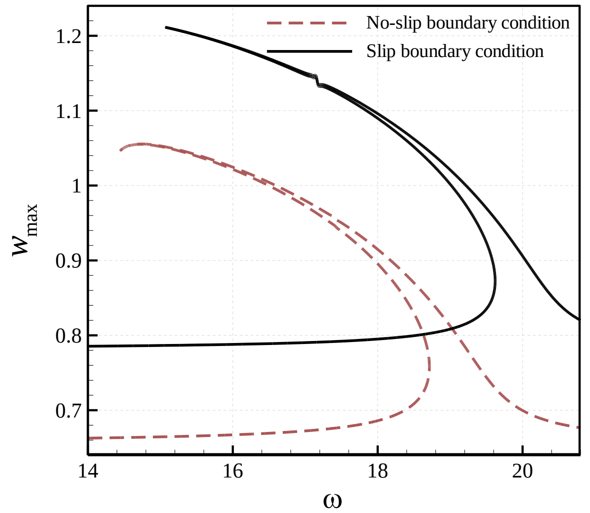


Fig. 8. Nonlinear frequency response of the nanosystem for slip and no-slip conditions for $w_{max}$ at $x$=0.5; $U$=6.50, $A_0$=0.15 and $F_1$=2.5

given. The discretisation of the motion equations was performed using Galerkin's technique, leading to a system of nonlinear ordinary differential equations. Then, a continuation method of solution was developed for solving the system of equations. The present modelling and methodology would be helpful for different nanoengineering applications such as ultrasmall pipettes, nanofluid filtration, drug delivery and nanofluidics.

Numerical results showed the importance of the effect of initial deflection on the frequency response of nanotubes conveying flow. For a slight initial deflection, the nanosystem displays a hardening-type frequency response. However, when the initial deflection is larger, the frequency response of the nanosystem is governed by a softening-hardening response. Furthermore, it was indicated that enhancing the nonlocal influence reduces the frequency parameter of ultrasmall tubes due to the reduction of their stiffness while boosting the strain gradient influence causes the opposite trend since it generally improves the tube stiffness. Moreover, modal interactions are substantially influenced by the initial deflection. The CT predicts higher resonance frequencies than the NSGT because of the decreasing influence of stress nonlocality on the stiffness. Furthermore, the CT is not reliable since it overestimates modal interactions. Slip condition effects greatly depend on the flow speed. For comparatively small flow speeds, slip effects reduce the resonance frequency. However, slip effects are linked with a noticeable increase in the resonance frequency of the nanosystem when the flow speed is higher.

## References


Ahouel, M., Houari, M.S.A., Bedia, E. and Tounsi, A. (2016), "Size-dependent mechanical behavior of functionally graded trigonometric shear deformable nanobeams including neutral surface position concept", *Steel Compos. Struct.*, **20**(5), 963-981. https://doi.org/10.12989/scs.2016.20.5.963.

Akgöz, B. and Civalek, Ö. (2011), "Buckling analysis of cantilever carbon nanotubes using the strain gradient elasticity and modified couple stress theories", *J. Comput. Theoretical Nanosci.*, **8**(9), 1821-1827.

Akgöz, B. and Civalek, Ö. (2013), "A size-dependent shear deformation beam model based on the strain gradient elasticity theory", *Int. J. Eng. Sci.*, **70**, 1-14. https://doi.org/10.1016/j.ijengsci.2013.04.004.

Akgöz, B. and Civalek, Ö. (2014), "Longitudinal vibration analysis for microbars based on strain gradient elasticity theory", *J. Vib. Control*, **20**(4), 606-616. https://doi.org/10.1177%2F1077546312463752.

Akgöz, B. and Civalek, Ö. (2017), "Effects of thermal and shear deformation on vibration response of functionally graded thick composite microbeams", *Compos. Part B Eng.*, **129**, 77-87. https://doi.org/10.1016/j.compositesb.2017.07.024.

Al-Basyouni, K., Tounsi, A. and Mahmoud, S. (2015), "Size dependent bending and vibration analysis of functionally graded micro beams based on modified couple stress theory and neutral surface position", *Compos. Struct.*, **125**, 621-630. https://doi.org/10.1016/j.compstruct.2014.12.070.

Amiri, A., Talebitooti, R. and Li, L. (2018), "Wave propagation in viscous-fluid-conveying piezoelectric nanotubes considering surface stress effects and Knudsen number based on nonlocal strain gradient theory", *Europe Phys. J. Plus*, **133**(7), 252. https://doi.org/10.1140/epjp/i2018-12077-y.

Arefi, M. (2019), "Static analysis of laminated piezo-magnetic size-dependent curved beam based on modified couple stress theory", *Struct. Eng. Mech.*, **69**(2), 145-153. https://doi.org/10.12989/sem.2019.69.2.145.

Asemi, S.R. and Farajpour, A. (2014), "Vibration characteristics of double-piezoelectric-nanoplate-systems", *IET Micro Nano Lett.*, **9**(4), 280-285. https://doi.org/10.1049/mnl.2013.0741.

Askari, H. and Esmailzadeh, E. (2017), "Forced vibration of fluid conveying carbon nanotubes considering thermal effect and nonlinear foundations", *Compos. Part B Eng.*, **113**, 31-43.

Bahaadini, R., Saidi, A.R. and Hosseini, M. (2018), "On dynamics of nanotubes conveying nanoflow", *Int. J. Eng. Sci.*, **123**, 181-196. https://doi.org/10.1016/j.ijengsci.2017.11.010.

Bakhadda, B., Bouiadjra, M.B., Bourada, F., Bousahla, A.A., Tounsi, A. and Mahmoud, S. (2018), "Dynamic and bending analysis of carbon nanotube-reinforced composite plates with elastic foundation", *Wind Struct.*, **27**(5), 311-324. https://doi.org/10.12989/was.2018.27.5.311.

Bedia, W.A., Houari, M.S.A., Bessaim, A., Bousahla, A.A., Tounsi, A., Saeed, T. and Alhodaly, M.S. (2019), "A New Hyperbolic Two-Unknown Beam Model for Bending and Buckling Analysis of a Nonlocal Strain Gradient Nanobeams", *J. Nano Res.*, **57**, 175-191. https://doi.org/10.4028/www.scientific.net/JNanoR.57.175.

Belkorissat, I., Houari, M.S.A., Tounsi, A., Bedia, E. and Mahmoud, S. (2015), "On vibration properties of functionally graded nano-plate using a new nonlocal refined four variable model", *Steel Compos. Struct*, **18**(4), 1063-1081. https://doi.org/10.12989/scs.2015.18.4.1063.

Bellifa, H., Benrahou, K.H., Bousahla, A.A., Tounsi, A. and Mahmoud, S. (2017), "A nonlocal zeroth-order shear deformation theory for nonlinear postbuckling of nanobeams", *Struct. Eng. Mech.*, **62**(6), 695-702. https://doi.org/10.12989/sem.2017.62.6.695.

Benahmed, A., Fahsi, B., Benzair, A., Zidour, M., Bourada, F. and Tounsi, A. (2019), "Critical buckling of functionally graded nanoscale beam with porosities using nonlocal higher-order shear deformation", *Struct. Eng. Mech.*, **69**(4), 457-466. https://doi.org/10.12989/sem.2019.69.4.457.

Besseghier, A., Houari, M.S.A., Tounsi, A. and Mahmoud, S. (2017), "Free vibration analysis of embedded nanosize FG plates using a new nonlocal trigonometric shear deformation theory", *Smart Struct. Syst.*, **19**(6), 601-614. https://doi.org/10.12989/sss.2017.19.6.601.

Bouadi, A., Bousahla, A.A., Houari, M.S.A., Heireche, H. and Tounsi, A. (2018), "A new nonlocal HSDT for analysis of stability of single layer graphene sheet", *Advances in nano research*, **6**(2), 147-162. https://doi.org/10.12989/anr.2018.6.2.147.

Bouafia, K., Kaci, A., Houari, M.S.A., Benzair, A. and Tounsi, A. (2017), "A nonlocal quasi-3D theory for bending and free flexural vibration behaviors of functionally graded nanobeams", *Smart Struct. Syst.*, **19**(2), 115-126. https://doi.org/10.12989/sss.2017.19.2.115.

Bounouara, F., Benrahou, K.H., Belkorissat, I. and Tounsi, A. (2016), "A nonlocal zeroth-order shear deformation theory for free vibration of functionally graded nanoscale plates resting on elastic foundation", *Steel Compos. Struct.*, **20**(2), 227-249. https://doi.org/10.12989/scs.2016.20.2.227.

Bourada, F., Amara, K., Bousahla, A.A., Tounsi, A. and Mahmoud, S. (2018), "A novel refined plate theory for stability analysis of hybrid and symmetric S-FGM plates", *Struct. Eng. Mech.*, **68**(6), 661-675. https://doi.org/10.12989/sem.2018.68.6.661.

Chaht, F.L., Kaci, A., Houari, M.S.A., Tounsi, A., Bég, O.A. and Mahmoud, S. (2015), "Bending and buckling analyses of functionally graded material (FGM) size-dependent nanoscale beams including the thickness stretching effect", *Steel Compos. Struct.*, **18**(2), 425-442. https://doi.org/10.12989/scs.2015.18.2.425.

Civalek, Ö. and Akgöz, B. (2013), "Vibration analysis of micro-scaled sector shaped graphene surrounded by an elastic matrix", *Comput. Mater. Sci.*, **77**, 295-303. https://doi.org/10.1016/j.commatsci.2013.04.055.

Demir, Ç. and Civalek, Ö. (2017), "A new nonlocal FEM via Hermitian cubic shape functions for thermal vibration of nano beams surrounded by an elastic matrix", *Compos. Struct.,* **168**, 872-884. https://doi.org/10.1016/j.compstruct.2017.02.091.

Demir, Ç. and Civalek, Ö. (2017), "On the analysis of microbeams", *Int. J. Eng. Sci.*, **121**, 14-33. https://doi.org/10.1016/j.ijengsci.2017.08.016.

Demir, Ç., Mercan, K. and Civalek, Ö. (2016), "Determination of critical buckling loads of isotropic, FGM and laminated truncated conical panel", *Compos. Part B Eng.*, **94**, 1-10. https://doi.org/10.1016/j.compositesb.2016.03.031.

Draoui, A., Zidour, M., Tounsi, A. and Adim, B. (2019), "Static and Dynamic Behavior of Nanotubes-Reinforced Sandwich

Plates Using (FSDT)", *J. Nano Res.*, **57**, 117-135. https://doi.org/10.4028/www.scientific.net/JNanoR.57.117.

Ebrahimi, F. and Barati, M.R. (2018), "A nonlocal strain gradient refined plate model for thermal vibration analysis of embedded graphene sheets via DQM", *Struct. Eng. Mech.*, **66**(6), 693-701. https://doi.org/10.12989/sem.2018.66.6.693.

Ebrahimi, F. and Dabbagh, A. (2018), "NSGT-based acoustical wave dispersion characteristics of thermo-magnetically actuated double-nanobeam systems", *Struct. Eng. Mech.*, **68**(6), 701-711. https://doi.org/10.12989/sem.2018.68.6.701.

Ebrahimi, F., Haghi, P. and Dabbagh, A. (2018), "Analytical wave dispersion modeling in advanced piezoelectric double-layered nanobeam systems", *Struct. Eng. Mech.*, **67**(2), 175-183. https://doi.org/10.12989/sem.2018.67.2.175.

Eringen, A.C. and Edelen, D. (1972), "On nonlocal elasticity", *Int. J. Eng. Sci.*, **10**(3), 233-248. https://doi.org/10.1016/0020-7225(72)90039-0.

Farajpour, A., Ghayesh, M.H. and Farokhi, H. (2018), "A review on the mechanics of nanostructures", *Int. J. Eng. Sci.*, **133**, 231-263. https://doi.org/10.1016/j.ijengsci.2018.09.006.

Farajpour, A., Ghayesh, M.H. and Farokhi, H. (2019), "Large-amplitude coupled scale-dependent behaviour of geometrically imperfect NSGT nanotubes", *J. Mech. Sci.*, **150**, 510-525. https://doi.org/10.1016/j.ijmecsci.2018.09.043.

Farajpour, A., Rastgoo, A. and Farajpour, M. (2017), "Nonlinear buckling analysis of magneto-electro-elastic CNT-MT hybrid nanoshells based on the nonlocal continuum mechanics", *Compos. Struct.*, **180**, 179-191. https://doi.org/10.1016/j.compstruct.2017.07.100.

Farajpour, M., Shahidi, A. and Farajpour, A. (2018), "A nonlocal continuum model for the biaxial buckling analysis of composite nanoplates with shape memory alloy nanowires", *Mater. Res. Exp.*, **5**(3), 035026. https://doi.org/10.1088/2053-1591/aab3a9.

Farajpour, M., Shahidi, A., Tabataba'i-Nasab, F. and Farajpour, A. (2018), "Vibration of initially stressed carbon nanotubes under magneto-thermal environment for nanoparticle delivery via higher-order nonlocal strain gradient theory", *Europe Phys. J. Plus*, **133**(6), 219. https://doi.org/10.1140/epjp/i2018-12039-5.

Farajpour, M.R., Shahidi, A.R., Tabataba'i-Nasab, F. and Farajpour, A. (2018), "Vibration of initially stressed carbon nanotubes under magneto-thermal environment for nanoparticle delivery via higher-order nonlocal strain gradient theory", *European Phys. J. Plus*, **133**(6), 219. https://doi.org/10.1140/epjp/i2018-12039-5.

Farajpour, M.R., Shahidi, A.R., Hadi, A. and Farajpour, A. (2019), "Influence of initial edge displacement on the nonlinear vibration, electrical and magnetic instabilities of magneto-electro-elastic nanofilms", *Mech. Adv. Mater. Struct*., **26**(17), 1469-1481. https://doi.org/10.1080/15376494.2018.1432820.

Farajpour, M.R., Shahidi, A.R. and Farajpour, A. (2019), "Influence of shear preload on wave propagation in small-scale plates with nanofibers", *Struct. Eng. Mech.*, **70**(4), 407-420. https://doi.org/10.12989/sem.2019.70.4.407.

Farajpour, A., Farokhi, H., Ghayesh, M.H. and Hussain, S. (2018), "Nonlinear mechanics of nanotubes conveying fluid", *J. Eng. Sci.*, **133**, 132-143. https://doi.org/10.1016/j.ijengsci.2018.08.009.

Farajpour, A., Ghayesh, M.H. and Farokhi, H. (2019), "Large-amplitude coupled scale-dependent behaviour of geometrically imperfect NSGT nanotubes", *J. Mech. Sci*., **150**, 510-525. https://doi.org/10.1016/j.ijmecsci.2018.09.043.

Farokhi, H. and Ghayesh, M.H. (2015), "Nonlinear dynamical behaviour of geometrically imperfect microplates based on modified couple stress theory", *J. Mech. Sci.*, **90**, 133-144. https://doi.org/10.1016/j.ijmecsci.2014.11.002.

Farokhi, H. and Ghayesh, M.H. (2018), "Nonlinear mechanical behaviour of microshells", *Int. J. Eng. Sci.*, **127**, 127-144. https://doi.org/10.1016/j.ijengsci.2018.02.009.

Farokhi, H. and Ghayesh, M.H. (2018), "Nonlinear mechanics of electrically actuated microplates", *Int. J. Eng. Sci.*, **123**, 197-213. https://doi.org/10.1016/j.ijengsci.2017.08.017.

Farokhi, H. and Ghayesh, M.H. (2018), "Supercritical nonlinear parametric dynamics of Timoshenko microbeams", *Communication Nonlinear Sci. Numeric. Simul.*, **59**, 592-605. https://doi.org/10.1016/j.cnsns.2017.11.033.

Farokhi, H., Ghayesh, M.H. and Hussain, S. (2016), "Large-amplitude dynamical behaviour of microcantilevers", *Int. J. Eng. Sci.*, **106**, 29-41. https://doi.org/10.1016/j.ijengsci.2016.03.002.

Farokhi, H. and Ghayesh, M.H. (2017), "Nonlinear resonant response of imperfect extensible Timoshenko microbeams", *J. Mech. Mater. Design*, **13**(1), 43-55. https://doi.org/10.1007/s10999-015-9316-z.

Farokhi, H., Ghayesh, M.H. and Gholipour, A. (2017), "Dynamics of functionally graded micro-cantilevers", *J. Eng. Sci*., **115**, 117-130. https://doi.org/10.1016/j.ijengsci.2017.01.004.

Filiz, S. and Aydogdu, M. (2015), "Wave propagation analysis of embedded (coupled) functionally graded nanotubes conveying fluid", *Compos. Struct.*, **132**, 1260-1273. https://doi.org/10.1016/j.compstruct.2015.07.043.

Gao, Y., Xiao, W.S. and Zhu, H. (2019), "Nonlinear vibration of functionally graded nano-tubes using nonlocal strain gradient theory and a two-steps perturbation method", *Struct. Eng. Mech.*, **69**(2), 205-219. https://doi.org/10.12989/sem.2019.69.2.205.

Ghayesh, M.H. (2018), "Dynamics of functionally graded viscoelastic microbeams", *Int. J. Eng. Sci.*, **124**, 115-131. https://doi.org/10.1016/j.ijengsci.2017.11.004.

Ghayesh, M.H. (2018), "Functionally graded microbeams: Simultaneous presence of imperfection and viscoelasticity", *J. Mech. Sci.*, **140**, 339-350. https://doi.org/10.1016/j.ijmecsci.2018.02.037.

Ghayesh, M.H. (2018), "Nonlinear vibration analysis of axially functionally graded shear-deformable tapered beams", *Applied Mathematical Modelling*, **59**, 583-596. https://doi.org/10.1016/j.apm.2018.02.017.

Ghayesh, M.H., Amabili, M. and Farokhi, H. (2013), "Nonlinear forced vibrations of a microbeam based on the strain gradient elasticity theory", *Int. J. Eng. Sci.*, **63**, 52-60. https://doi.org/10.1016/j.ijengsci.2012.12.001.

Ghayesh, M.H., Amabili, M. and Farokhi, H. (2013), "Three-dimensional nonlinear size-dependent behaviour of Timoshenko microbeams", *Int. J. Eng. Sci.*, **71**, 1-14. https://doi.org/10.1016/j.ijengsci.2013.04.003.

Ghayesh, M.H. and Farajpour, A. (2018), "Nonlinear mechanics of nanoscale tubes via nonlocal strain gradient theory", *Int. J. Eng. Sci.*, **129**, 84-95. https://doi.org/10.1016/j.ijengsci.2018.04.003.

Ghayesh, M.H. and Farokhi, H. (2015), "Chaotic motion of a parametrically excited microbeam", *Int. J. Eng. Sci.*, **96**, 34-45. https://doi.org/10.1016/j.ijengsci.2015.07.004.

Ghayesh, M.H., Farokhi, H. and Alici, G. (2016), "Size-dependent performance of microgyroscopes", *Int. J. Eng. Sci.*, **100**, 99-111. https://doi.org/10.1016/j.ijengsci.2015.11.003.

Gholipour, A., Farokhi, H. and Ghayesh, M.H. (2015), "In-plane and out-of-plane nonlinear size-dependent dynamics of microplates", *Nonlinear Dynam.*, **79**(3), 1771-1785. https://doi.org/10.1007/s11071-014-1773-7.

Ghayesh, M.H., Farokhi, H. and Alici, G. (2015), "Subcritical parametric dynamics of microbeams", *J. Eng. Sci*., **95**, 36-48. https://doi.org/10.1016/j.ijengsci.2015.06.001.

Ghayesh, M.H. (2012), "Subharmonic dynamics of an axially accelerating beam", *Archive Appl. Mech.*, **82**(9), 1169-1181. https://doi.org/10.1007/s00419-012-0609-5.

Ghayesh, M.H. and Farajpour, A. (2019), "A review on the mechanics of functionally graded nanoscale and microscale structures", *J. Eng. Sci*., **137**, 8-36. https://doi.org/10.1016/j.ijengsci.2018.12.001.

Ghayesh, M.H., Farokhi, H. and Farajpour, A. (2019), "Global dynamics of fluid conveying nanotubes", *J. Eng. Sci.*, **135**, 37-57. https://doi.org/10.1016/j.ijengsci.2018.11.003.

Hamza-Cherif, R., Meradjah, M., Zidour, M., Tounsi, A., Belmahi, S. and Bensattalah, T. (2018), "Vibration analysis of nano beam using differential transform method including thermal effect", *J. Nano Res.*, **54**, 1-14. https://doi.org/10.4028/www.scientific.net/JNanoR.54.1.

Kadari, B., Bessaim, A., Tounsi, A., Heireche, H., Bousahla, A.A. and Houari, M.S.A. (2018), "Buckling analysis of orthotropic nanoscale plates resting on elastic foundations", *J. Nano Res.*, **55**, 42-56. https://doi.org/10.4028/www.scientific.net/JNanoR.55.42.

Karami, B., Janghorban, M., Shahsavari, D. and Tounsi, A. (2018), "A size-dependent quasi-3D model for wave dispersion analysis of FG nanoplates", *Steel Compos. Struct.*, **28**(1), 99-110. https://doi.org/10.12989/scs.2018.28.1.099.

Karami, B., Janghorban, M. and Tounsi, A. (2017), "Effects of triaxial magnetic field on the anisotropic nanoplates", *Steel Compos. Struct.*, **25**(3), 361-374. https://doi.org/10.12989/scs.2017.25.3.361.

Karami, B., Janghorban, M. and Tounsi, A. (2018), "Galerkin's approach for buckling analysis of functionally graded anisotropic nanoplates/different boundary conditions", *Eng. Comput.*, 1-20. https://doi.org/10.1007/s00366-018-0664-9.

Karami, B., Janghorban, M. and Tounsi, A. (2018), "Nonlocal strain gradient 3D elasticity theory for anisotropic spherical nanoparticles", *Steel Compos. Struct.*, **27**(2), 201-216. https://doi.org/10.12989/scs.2018.27.2.201.

Karami, B., Janghorban, M. and Tounsi, A. (2018), "Variational approach for wave dispersion in anisotropic doubly-curved nanoshells based on a new nonlocal strain gradient higher order shell theory", *Thin-Walled Struct.*, **129**, 251-264. https://doi.org/10.1016/j.tws.2018.02.025.

Karami, B., Janghorban, M. and Tounsi, A. (2019), "On exact wave propagation analysis of triclinic material using three-dimensional bi-Helmholtz gradient plate model", *Struct. Eng. Mech.*, **69**(5), 487-497. https://doi.org/10.12989/sem.2019.69.5.487.

Karami, B., Shahsavari, D., Janghorban, M. and Tounsi, A. (2019), "Resonance behavior of functionally graded polymer composite nanoplates reinforced with graphene nanoplatelets", *J. Mech. Sci.*, **156**, 94-105. https://doi.org/10.1016/j.ijmecsci.2019.03.036

Kazemirad, S., Ghayesh, M.H. and Amabili, M. (2013), "Thermo-mechanical nonlinear dynamics of a buckled axially moving beam", *Archive Appl. Mech.*, **83**(1), 25-42. https://doi.org/10.1007/s00419-012-0630-8.

Khetir, H., Bouiadjra, M.B., Houari, M.S.A., Tounsi, A. and Mahmoud, S. (2017), "A new nonlocal trigonometric shear deformation theory for thermal buckling analysis of embedded nanosize FG plates", *Struct. Eng. Mech.*, **64**(4), 391-402. https://doi.org/10.12989/sem.2017.64.4.391.

Li, X., Li, L., Hu, Y., Ding, Z. and Deng, W. (2017), "Bending, buckling and vibration of axially functionally graded beams based on nonlocal strain gradient theory", *Compos. Struct.*, **165**, 250-265. https://doi.org/10.1016/j.compstruct.2017.01.032.

Liang, F. and Su, Y. (2013), "Stability analysis of a single-walled carbon nanotube conveying pulsating and viscous fluid with nonlocal effect", *Appl. Math. Modell.*, **37**(10-11), 6821-6828. https://doi.org/10.1016/j.apm.2013.01.053.

Lim, C., Zhang, G. and Reddy, J. (2015), "A higher-order nonlocal elasticity and strain gradient theory and its applications in wave propagation", *J. Mech. Phys. Solid.*, **78**, 298-313. https://doi.org/10.1016/j.jmps.2015.02.001.

Malekzadeh, P., Haghighi, M.G. and Shojaee, M. (2014), "Nonlinear free vibration of skew nanoplates with surface and small scale effects", *Thin Wall Struct.*, **78**, 48-56. https://doi.org/10.1016/j.tws.2013.10.027.

Malekzadeh, P. and Shojaee, M. (2015), "A two-variable first-order shear deformation theory coupled with surface and nonlocal effects for free vibration of nanoplates", *J. Vib. Control*, **21**(14), 2755-2772. https://doi.org/10.1177/1077546313516667.

Malekzadeh, P. and Farajpour, A. (2012), "Axisymmetric free and forced vibrations of initially stressed circular nanoplates embedded in an elastic medium", *Acta Mechanica*, **223**(11), 2311-2330. https://doi.org/10.1007/s00707-012-0706-0.

Malikan, M. (2017), "Electro-mechanical shear buckling of piezoelectric nanoplate using modified couple stress theory based on simplified first order shear deformation theory", *Appl. Math. Modell.*, **48**, 196-207. https://doi.org/10.1016/j.apm.2017.03.065.

Maraghi, Z.K., Arani, A.G., Kolahchi, R., Amir, S. and Bagheri, M. (2013), "Nonlocal vibration and instability of embedded DWBNNT conveying viscose fluid", *Compos. Part B Eng.*, **45**(1), 423-432. https://doi.org/10.1016/j.compositesb.2012.04.066.

Mercan, K. and Civalek, Ö. (2016), "DSC method for buckling analysis of boron nitride nanotube (BNNT) surrounded by an elastic matrix", *Compos. Struct.*, **143**, 300-309. https://doi.org/10.1016/j.compstruct.2016.02.040.

Mercan, K. and Civalek, Ö. (2017), "Buckling analysis of Silicon carbide nanotubes (SiCNTs) with surface effect and nonlocal elasticity using the method of HDQ", *Compos. Part B Eng.*, **114**, 34-45. https://doi.org/10.1016/j.compositesb.2017.01.067.

Mohammadi, M. and Rastgoo, A. (2019), "Nonlinear vibration analysis of the viscoelastic composite nanoplate with three directionally imperfect porous FG core", *Struct. Eng. Mech.*, **69**(2), 131-143. https://doi.org/10.12989/sem.2019.69.2.131.

Mohammadi, M., Farajpour, A., Goodarzi, M. and Heydarshenas, R. (2013), "Levy type solution for nonlocal thermo-mechanical vibration of orthotropic mono-layer graphene sheet embedded in an elastic medium", *J. Solid Mech.*, **5**(2), 116-132.

Mohammadi, M., Farajpour, A., Goodarzi, M., Dinari, F. (2014), "Thermo-mechanical vibration analysis of annular and circular graphene sheet embedded in an elastic medium", Latin American J. Solids Struct., **11**(4), 659-682. http://dx.doi.org/10.1590/S1679-78252014000400007.

Mokhtar, Y., Heireche, H., Bousahla, A.A., Houari, M.S.A., Tounsi, A. and Mahmoud, S. (2018), "A novel shear deformation theory for buckling analysis of single layer graphene sheet based on nonlocal elasticity theory", *Smart Struct. Syst.*, **21**(4), 397-405. https://doi.org/10.12989/sss.2018.21.4.397.

Mouffoki, A., Bedia, E., Houari, M.S.A., Tounsi, A. and Mahmoud, S. (2017), "Vibration analysis of nonlocal advanced nanobeams in hygro-thermal environment using a new two-unknown trigonometric shear deformation beam theory", *Smart Struct. Syst.*, **20**(3), 369-383. https://doi.org/10.12989/sss.2017.20.3.369.

Murmu, T. and Adhikari, S. (2013), "Nonlocal mass nanosensors based on vibrating monolayer graphene sheets", *Sensor Actuator B Chem.*, **188**, 1319-1327. https://doi.org/10.1016/j.snb.2013.07.051.

Nebab, M., Atmane, H.A., Bennai, R., Tounsi, A. and Adda Bedia, E.A. (2019), "Vibration response and wave propagation in FG plates resting on elastic foundations using HSDT", *Struct. Eng. Mech.*, **69**(5), 511-525. https://doi.org/10.12989/sem.2019.69.5.511.

Nejad, M.Z., Hadi, A. and Farajpour, A. (2017), "Consistent couple-stress theory for free vibration analysis of Euler-Bernoulli nano-beams made of arbitrary bi-directional functionally graded materials", *Struct. Eng. Mech.*, **63**(2), 161-169. https://doi.org/10.12989/sem.2017.63.2.161.

Nejad, M.Z., Hadi, A., Omidvari, A. and Rastgoo, A. (2018), "Bending analysis of bi-directional functionally graded Euler-Bernoulli nano-beams using integral form of Eringen's non-local elasticity theory", *Struct. Eng. Mech.*, **67**(4), 417-425.

Numanoğlu, H.M., Akgöz, B. and Civalek, Ö. (2018), "On dynamic analysis of nanorods", *Int. J. Eng. Sci.*, **130**, 33-50. https://doi.org/10.1016/j.ijengsci.2018.05.001.

Paidoussis, M.P. (1998), *Fluid-structure interactions: slender structures and axial flow*, Academic press, MA, USA.

Peddieson, J., Buchanan, G.R. and McNitt, R.P. (2003), "Application of nonlocal continuum models to nanotechnology", *Int. J. Eng. Sci.*, **41**(3-5), 305-312. https://doi.org/10.1016/S0020-7225(02)00210-0.

Rahmani, O., Refaeinejad, V. and Hosseini, S. (2017), "Assessment of various nonlocal higher order theories for the bending and buckling behavior of functionally graded nanobeams", *Steel Compos. Struct*, **23**(3), 339-350. https://doi.org/10.12989/scs.2017.23.3.339.

Reddy, J. (2010), "Nonlocal nonlinear formulations for bending of classical and shear deformation theories of beams and plates", *Int. J. Eng. Sci.*, **48**(11), 1507-1518. https://doi.org/10.1016/j.ijengsci.2010.09.020.

Romano, G., Barretta, R. and Diaco, M. (2017), "On nonlocal integral models for elastic nano-beams", *J. Mech. Sci.*, **131**, 490-499. https://doi.org/10.1016/j.ijmecsci.2017.07.013.

Semmah, A., Heireche, H., Bousahla, A.A. and Tounsi, A. (2019), "Thermal buckling analysis of SWBNNT on Winkler foundation by non local FSDT", *Adv. Nano Res.*, **7**(2), 89-98. https://doi.org/10.12989/anr.2019.7.2.089.

Shen, H.-S. (2011), "Nonlinear analysis of lipid tubules by nonlocal beam model", *J. Theoretical Bio.*, **276**(1), 50-56. https://doi.org/10.1016/j.jtbi.2011.02.001.

Şimşek, M. (2016), "Nonlinear free vibration of a functionally graded nanobeam using nonlocal strain gradient theory and a novel Hamiltonian approach", *Int. J. Eng. Sci.*, **105**, 12-27. https://doi.org/10.1016/j.ijengsci.2016.04.013.

Şimşek, M. and Reddy, J. (2013), "Bending and vibration of functionally graded microbeams using a new higher order beam theory and the modified couple stress theory", *Int. J. Eng. Sci.*, **64**, 37-53. https://doi.org/10.1016/j.ijengsci.2012.12.002.

Soltani, P., Taherian, M. and Farshidianfar, A. (2010), "Vibration and instability of a viscous-fluid-conveying single-walled carbon nanotube embedded in a visco-elastic medium", *J. Phys. D Appl. Phys.*, **43**(42), 425401. https://doi.org/10.1088/0022-3727/43/42/425401.

Tlidji, Y., Zidour, M., Draiche, K., Safa, A., Bourada, M., Tounsi, A., Bousahla, A.A. and Mahmoud, S. (2019), "Vibration analysis of different material distributions of functionally graded microbeam", *Struct. Eng. Mech.*, **69**(6), 637-649. https://doi.org/10.12989/sem.2019.69.6.637.

Tounsi, A., Heireche, H., Berrabah, H., Benzair, A. and Boumia, L. (2008), "Effect of small size on wave propagation in double-walled carbon nanotubes under temperature field", *J. Appl. Phys.,* **104**(10), 104301. https://doi.org/10.1063/1.3018330.

Wang, Y.-Z., Li, F.-M. and Kishimoto, K. (2010), "Wave propagation characteristics in fluid-conveying double-walled nanotubes with scale effects", *Comput. Mater. Sci.*, **48**(2), 413-418. https://doi.org/10.1016/j.commatsci.2010.01.034.

Yazid, M., Heireche, H., Tounsi, A., Bousahla, A.A. and Ahmed Houari, M.S. (2018), "A novel nonlocal refined plate theory for stability response of orthotropic single-layer graphene sheet resting on elastic medium", *Smart Struct. Syst.*, **21**(1), 15-25. https://doi.org/10.12989/sss.2018.21.1.015.

Youcef, D.O., Kaci, A., Benzair, A., Bousahla, A.A. and Tounsi, A. (2018), "Dynamic analysis of nanoscale beams including surface stress effects", *Smart Struct. Syst.*, **21**(1), 65-74. https://doi.org/10.12989/sss.2018.21.1.065.

Zenkour, A. and Sobhy, M. (2013), "Nonlocal elasticity theory for thermal buckling of nanoplates lying on Winkler–Pasternak elastic substrate medium", *Physica E Low-dimensional Syst. Nanostruct.*, **53**, 251-259. https://doi.org/10.1016/j.physe.2013.04.022.

Zhang, B., He, Y., Liu, D., Gan, Z. and Shen, L. (2014), "Non-classical Timoshenko beam element based on the strain gradient elasticity theory", *Finite Elements Anal. Design*, **79**, 22-39. https://doi.org/10.1016/j.finel.2013.10.004.

*PL*